Identification of a Potential Biomarker for FABP4 Inhibition: The Power of Lipidomics in Preclinical Drug Testing

KARSTEN SUHRE,[1,2] WERNER RÖMISCH-MARGL,[1] MARTIN HRABÉ DE ANGELIS,[3,4] JERZY ADAMSKI,[3,4] GERD LUIPPOLD,[5] and ROBERT AUGUSTIN[5]

The fatty acid binding protein 4 (FABP4) belongs to the family of lipid chaperones that control intracellular fluxes and compartmentalization of their respective ligands (e.g., fatty acids). FABP4, which is almost exclusively expressed in adipocytes and macrophages, contributes to the development of insulin resistance and atherosclerosis in mice. Lack of FABP4 protects against the development of insulin resistance associated with genetic or diet-induced obesity in mice. Furthermore, total or macrophage-specific FABP4 deficiency is protective against atherosclerosis in apolipoprotein E–deficient mice. The FABP4 small-molecule inhibitor BMS309403 has demonstrated efficacy in mouse models for type 2 diabetes mellitus and atherosclerosis, resembling phenotypes of mice with FABP4 deficiency. However, despite the therapeutically attractive long-term effects of FABP4 inhibition, an acute biomarker for drug action is lacking. The authors applied mass spectrometry lipidomics analysis to in vitro and in vivo (plasma and adipose tissue) samples upon inhibitor treatment. They report the identification of a potential biomarker for acute in vivo FABP4 inhibition that is applicable for further investigations and can be implemented in simple and fast-flow injection mass spectrometry assays. In addition, this approach can be considered a proof-of-principle study that can be applied to other lipid-pathway targeting mechanisms. (*Journal of Biomolecular Screening* 2011;16:467-475)

Key words: type 2 diabetes, atherosclerosis, fatty acid binding protein, metabolomics, mass spectroscopy, drug action, biomarkers

INTRODUCTION

LIPIDS AND THEIR RESPECTIVE SIGNALS are causally involved and critical in the pathogenesis of type 2 diabetes (T2D) and atherosclerosis.[1-4] Fatty acid–binding proteins (FABPs), small (14−15 kDa) cytosolic proteins, bind hydrophobic ligands (e.g., saturated and unsaturated long-chain fatty acids, eicosanoids, leukotrienes, and prostaglandins).[5] FABPs have been implicated in shuttling their respective ligands to different subcellular compartments such as mitochondria, nuclei, endoplasmic reticulum (ER), and lipid droplets, thereby modulating intracellular and extracellular lipid fluxes and effecting a range of cellular processes such as transcription and lipolysis.[5] FABP4 (also aP2; A-FABP) is highly expressed in adipocytes and macrophages. FABP4-deficient mice have demonstrated the significance of FABP4 in different aspects of impaired energy and lipid homeostasis. FABP4 knockout mice are partially protected against insulin resistance associated with diet or genetically induced obesity.[6,7] Furthermore, FABP4 plays an important role in lipid homeostasis and signaling in macrophages.[8] Total or macrophage-specific knockout has been shown to be protective against early and advanced atherosclerosis in a mouse model for atherosclerosis, the ApoE-deficient mice.[9]

The beneficial effects of FABP4 seen in mice models for T2D and atherosclerosis make FABP4 an interesting potential therapeutic target for intervention.[5] Small-molecule inhibitors for FABP4 have been actively pursued as potential therapeutics for treating T2D.[10,11] The recent description of the potent and selective FABP4 inhibitor BMS309403 that showed in vivo efficacy in mouse models for T2D and atherosclerosis demonstrated the feasibility of such a pharmacological approach.[12]

Thus far, the mode of action for FABP4 inhibition is incompletely understood,[5] and a mechanistic marker that allows

[1]Institute for Bioinformatics and Systems Biology, Helmholtz Zentrum München, German Research Center for Environmental Health, Neuherberg, Germany.
[2]Faculty of Biology, Ludwig-Maximilians-Universität, Planegg-Martinsried, Germany.
[3]Institute of Experimental Genetics, Genome Analysis Center, Helmholtz Zentrum München, German Research Center for Environmental Health, Neuherberg, Germany.
[4]Institute of Experimental Genetics, Life and Food Science Center Weihenstephan, Technische Universität München, Freising-Weihenstephan, Germany.
[5]Department of Cardiometabolic Diseases Research, Boehringer Ingelheim Pharma GmbH &Co KG, Biberach a.d. Riss, Germany.

characterization of potent FABP4 inhibitors and their efficacy in cellular systems and, more important, acutely in vivo is lacking. The recent identification of palmitoleate (16:1Δ7) as a "lipokine" in plasma samples from FABP4- and FABP5-deficient mice has indicated that alterations in lipid homeostasis due to deficiency of two fatty acid–binding proteins can be detected systemically.[13] We hypothesized that a metabolite in the FABP pathway should constitute a potential mechanistic marker that would allow differentiating potent inhibitors for their in vivo as well as in vitro efficacy. Therefore, aiming to identify biomarkers for FABP4 inhibition, we applied a robust and high-throughput-capable flow injection mass spectrometry–based lipidomics approach, with emphasis on an acute in vivo systemic readout.

The approach we present here consists of the application of a targeted lipidomics screen for many lipid species that are susceptible to be influenced by the action of a lipid-pathway targeting drug, both in established in vitro cell culture and in an in vivo animal model. In addition to our primary goal to establish an efficient mechanistic assay for FABP4 inhibition, we view this study as a prototype for future applications on related targets.

MATERIALS AND METHODS

Cell culture, differentiation of THP-1 monocytes and 3T3L1 fibroblasts, and treatment with the FABP4 inhibitor BMS309403

Human monocytic leukemia THP-1 cells (ATCC, Manassas, VA) were cultured in RPMI 1640 (#BE12-702F; Lonza, Basel, Switzerland) supplemented with 10% heat-inactivated fetal calf serum (FCS; Biological Industries, Kibbutz Beit-Haemek, Israel) at 37 °C in 5% CO_2. THP-1 monocytes were differentiated into macrophages with 100 ng/mL phorbol 12-myristate 13-acetate (PMA; #P1585; Sigma-Aldrich, St Louis, MO) for 48 h. After 48 h of PMA-induced differentiation, THP-1 macrophages were incubated in HL-1 medium (#77201; Lonza) with 100 ng/ mL PMA with different concentrations of the inhibitor dissolved in DMSO for 24 h. 3T3-L1 (#CL-173) fibroblasts were cultured in Dulbecco's modified Eagle's medium (DMEM; #BE12-604F; Lonza) with 10% fetal calf serum. Differentiation of 3T3-L1 fibroblasts into adipocytes was initiated 2 days postconfluence by changing the medium to DMEM supplemented with 10% FCS, 0.5 μM dexamethasone, 1.67 μM insulin (#I-5500; Sigma-Aldrich), 0.5 mM isobutylmehtylxanthine (#I-5879; Sigma-Aldrich), and 1 μM rosiglitazone. After 48 h, the cells were grown in DMEM with 10% FCS and 1.67 μM insulin for another 2 days and maintained in DMEM with 10% FCS until 9 days after initiation of differentiation. On day 9 after differentiation, 3T3L1 adipocytes were treated for 24 h with different concentrations of the FABP4 inhibitor applied under serum-free cell culture media conditions using HL-1 medium. Cell pellets from inhibitor-treated THP-1 macrophages and 3T3L1 adipocytes were subsequently subjected to lipidomics analysis.

Determination of MCP-1 secretion from THP-1 macrophages

Differentiation of THP-1 monocytes to macrophages was achieved as described above. Treatment was performed for 24 h with the inhibitor in HL-1 medium with different concentrations of FCS (0.2%, 5%, and 10%). Cell culture supernatants were removed, and amounts of secreted MCP-1 were quantified by enzyme-linked immunosorbent assay (ELISA; #555179; BD Pharmingen, San Diego, CA) and normalized per mg protein (BCA; #23225; Pierce, Rockford, IL).

In vivo experiments

All animal studies were approved by the Regierungspräsidium Tübingen and complied with the German Animal Protection Act (2006). A discovery–replication study design was implemented. In the discovery experiment, male ob/ob mice (B6.V-Lep[ob]/JBomTac) at the age of 7 to 8 weeks were randomized based on body weight (mean per group, 45.1 g; range, 41.9-50.4 g), and 14 animals per group were orally gavaged twice daily with vehicle, 40 mg/kg or 100 mg/kg of BMS309403, respectively. BMS309403 was dissolved in 10% 1-methyl-2-pyrrolidone, 5% cremophor, and 2% ethanol as described.[12] The application volume was 2 mL/kg. Blood and tissue samples were obtained at the second day of treatment 1 ($n = 7$) and 3 hours ($n = 7$) postdosing in the morning by sacrificing the animals by cervical dislocation. In the replication experiment, animals ($n = 10$) were treated as described above. However, blood sampling and removal of adipose tissue were performed on the second day of treatment only 2 hours postdosing in the morning. In addition, a second vehicle control (0.5% natrosol) was included. Age of the animals was 9 to 10 weeks, and mean body weight per group was 50.6 g, with a range of 47.8 to 53.3 g. Blood and epididymal adipose tissue samples were collected. Blood was centrifuged at 2000 g for 10 min at room temperature and EDTA plasma as well as adipose tissue frozen at −80 °C. The pharmacokinetic (PK) profile for the FABP4 inhibitor BMS309403 was determined using the dose of 40 mg/ kg orally administered to male 7- to 8-week-old ob/ob mice (n = 3; mean body weight, 47.9 g). The strain and age of the animals used in the present experiments were similar to the strain in which antidiabetic effects after treatment with BMS309403 could be shown.[12] Animals were provided by Taconic (Ry, Denmark).

Metabolite panel

The AbsoluteIDQ kit (BIOCRATES Life Sciences AG, Innsbruck, Austria) was used for metabolite analysis. This mass spectrometry–based metabolomics kit is a research assay identifying and quantifying in total 163 different metabolites (**Supplemental Tables 1** and **2**). The particular advantage of

this kit resides in the combination of rapid flow injection mass spectrometry (FIA-MS) with targeted multiple-reaction monitoring (MRM) and isotope-labeled quantification. Lipid side chain composition is abbreviated as Cx:y, where x denotes the number of carbons in the side chain and y the number of double bonds. For example, "PC ae C33:1" denotes an acyl-alkyl phosphatidylcholine with 33 carbons in the two fatty acid side chains and a single double bond in one of them. Full biochemical names are provided in **Supplemental Table 2**. The precise position of the double bonds and the distribution of the carbon atoms in different fatty acid side chains cannot be determined with this technology. In some cases, the mapping of metabolite names to individual masses can be ambiguous. For example, stereochemical differences are not always discernible; neither are isobaric fragments. In such cases, possible alternative assignments are indicated.

Metabolite extraction

Blood. EDTA plasma samples were vortexed after thawing and centrifuged at 4 °C for 5 min at 10 000 g before 10 µL of the supernatants was loaded onto the 96-well kit plate. Processing of the AbsoluteIDQ kit followed the manufacturer's manual and included following automated steps on a Hamilton ML Star robotics platform (Hamilton Bonaduz AG, Bonaduz, Switzerland): (1) drying of the plasma samples under a nitrogen stream, (2) derivatization of amino acids with 5% phenylisothiocyanate reagent (20 µL), (3) drying of samples, (4) extraction of metabolites and kit internal standards with 5 mM ammonium acetate in methanol (300 µL), (5) centrifugation through a filter plate (2 min, 500 g), and (6) dilution with 600 µL MS running solvent. Then, 20 µL of the final extracts was applied to FIA-MS.[14,15]

Epididymal adipose tissue. Adipose tissue was homogenized using a Precellys 24 homogenizer (PEQLAB Biotechnologie GmbH, Erlangen, Germany). The system was recently described for several MS and nuclear magnetic resonance (NMR) applications.[16-18] Frozen adipose tissue samples (50−100 mg) were placed into precooled (dry ice) 2-mL homogenization tubes containing ceramic beads (1.4 mm diameter). Precooled extraction solvent (MeOH) was added (3 µL/mg tissue), and the tissue was homogenized with the Precellys 24 homogenizer in three cycles, each 20 s, 5500 rpm, with 30-s cooling intervals between the homogenization steps. The tubes were subsequently centrifuged for 5 min at 10 000 g, and 10 µL of the supernatants was loaded onto the 96-well kit plate. The kit was processed as described above.

Cell culture. Cell pellets were resuspended in 200 µL ice-cold methanol and subjected to sonication (5 × 15 s, 30-s cooling in an ice bath between the cycles, ultrasonic cleaner USC300T;

VWR International GmbH, Darmstadt, Germany). The tubes were subsequently centrifuged for 5 min at 10 000 g, and 20 µL of the supernatants was loaded onto the kit plate. The kit was processed as described above.

Metabolite measurements

Plasma samples (100 µL) were processed with a Hamilton Star (Hamilton Bonaduz AG, Bonaduz, Switzerland) robot and prepared for quantification using the AbsoluteIDQ kit (BIOCRATES Life Sciences AG). Measurements were done on API 4000 Q TRAP LC/MS/MS System (Applied Biosystems, Darmstadt, Germany) equipped with a Schimadzu Prominence LC20AD pump and a SIL-20AC autosampler. The initial data preparation was performed using the MetIQ software package, which is an integral part of the AbsoluteIDQ kit as described.[19] Briefly, targeted metabolomics was used to quantitatively screen for known small-molecule metabolites using MRM, neutral loss, and precursor ion scans. Quantification of the metabolites of the biological sample was achieved by reference to appropriate internal standards. The method has been proven to be in conformance with 21CFR (Code of Federal Regulations) Part 11, which implies proof of reproducibility within a given error range (for coefficients of variation [CVs], see **Supplemental Table 2**). It has been applied in different academic and industrial applications.[14,15,20,21] Concentrations of all analyzed metabolites are reported in µM.

Statistical analysis

Association between dosage and each of the 163 metabolite concentrations was tested. No further adjustment was performed. R (version 2.6) and SPSS for Windows (Version 17.0; SPSS, Inc., an IBM Company, Chicago, IL) were used for statistical analysis. Motivated by our previous observation that the use of ratios may lead to a strong reduction in the overall variance and a corresponding improvement in the *p*-values of association,[20] we also computed all possible pairs of metabolite concentration ratios for those cases and used those ratios as quantitative traits (163*162 = 26.406 traits). In the discovery study, a linear regression model with interaction terms on the factors "time of sampling after gavage" (two levels: 1 h or 3 h) and "dosage" (metric variable: 0, 40, 100 mg/kg) was used. In the replication study and studies in cell culture and tissue samples, a linear regression with the dosage factor (metric variable: 0 [vehicle 2], 40, 100 mg/kg) was applied. Vehicle 1 was not used in the statistical analysis to avoid overweighting of the controls but served to validate the independence of the results on the type of vehicle (negative results not shown). To correct for testing all possible ratios between metabolite pairs for association, we computed the positive false discovery rate (*q*-value) following Storey[22] (**Table 1**). Moreover, it should be noted that

Table 1. Metabolite Ratios That Present a Positive Association with BMS309403 Dosage

Numerator	Denominator	p-Value	p-Value Replicate	q-Value	q-Value Replicate	R^2	R^2 Replicate
SM C16:0	PC ae C38:4	2.4×10^{-12}	9.6×10^{-11}	2.6×10^{-9}	2.5×10^{-7}	0.704	0.774
SM C16:0	PC aa C38:4	8.1×10^{-10}	5.5×10^{-10}	1.3×10^{-7}	5.1×10^{-7}	0.605	0.744
SM C18:1	PC aa C38:4	3.5×10^{-12}	9.0×10^{-10}	2.8×10^{-9}	6.9×10^{-7}	0.699	0.735
PC aa C32:0	PC aa C36:4	2.2×10^{-10}	5.8×10^{-9}	4.7×10^{-8}	2.8×10^{-6}	0.630	0.697
SM C18:1	PC aa C38:5	2.6×10^{-8}	7.0×10^{-9}	1.4×10^{-6}	2.8×10^{-6}	0.532	0.693
SM C18:0	PC aa C38:5	2.2×10^{-11}	1.7×10^{-8}	1.0×10^{-8}	4.9×10^{-6}	0.669	0.674
PC ae C34:1	PC ae C38:4	4.7×10^{-9}	2.2×10^{-8}	4.5×10^{-7}	5.8×10^{-6}	0.570	0.667
SM C16:0	PC ae C40:4	1.6×10^{-13}	2.9×10^{-8}	5.4×10^{-10}	6.4×10^{-6}	0.742	0.661
PC aa C30:0	PC ae C40:4	7.0×10^{-9}	2.9×10^{-8}	5.7×10^{-7}	6.4×10^{-6}	0.561	0.661
SM C18:0	PC aa C38:4	2.4×10^{-14}	4.0×10^{-8}	2.4×10^{-10}	7.4×10^{-6}	0.764	0.653
SM C18:0	PC aa C36:4	3.1×10^{-9}	4.8×10^{-8}	3.5×10^{-7}	8.2×10^{-6}	0.578	0.649
SM C16:1	PC aa C38:4	8.6×10^{-10}	1.4×10^{-7}	1.3×10^{-7}	1.6×10^{-5}	0.604	0.621
SM C18:0	PC ae C38:4	7.1×10^{-12}	1.8×10^{-7}	4.6×10^{-9}	1.9×10^{-5}	0.688	0.614
SM C16:0	PC ae C38:3	1.3×10^{-11}	2.8×10^{-7}	6.7×10^{-9}	2.4×10^{-5}	0.678	0.603
PC aa C30:2	PC aa C38:4	1.2×10^{-8}	2.9×10^{-7}	8.7×10^{-7}	2.5×10^{-5}	0.548	0.602
PC aa C32:0	PC ae C38:4	9.0×10^{-12}	3.8×10^{-7}	5.2×10^{-9}	2.9×10^{-5}	0.684	0.594
SM C18:1	lysoPC a C20:3	1.2×10^{-8}	4.7×10^{-7}	8.4×10^{-7}	3.3×10^{-5}	0.550	0.588

Reported are the strongest replicated associations (associations with a negative trend correspond to inverse ratios and do not carry additional information). Full metabolite names and % coefficients of variation are provided in **Supplemental Tables 1** and **2**. *p*-Values are calculated using a linear regression model; *q*-values are calculated following Storey.[22] The corresponding correlation coefficient R^2 is reported; data from the initial discovery study and the replication study are presented (see also **Fig. 2A,B**).

all associations are significant even after applying the more conservative Bonferroni correction, which requires in our cases *p*-values to be smaller than $p_{\text{Bonferroni}} = 0.05/(163*162) = 1.89 \times 10^{-6}$. In the replication experiment, one would in principle only have to correct for 17 traits tested. As in both experiments the level of significance is clearly below the Bonferroni threshold (the largest *p*-value in **Table 1** is $p = 4.7 \times 10^{-7}$), our associations are without any doubt true positives.
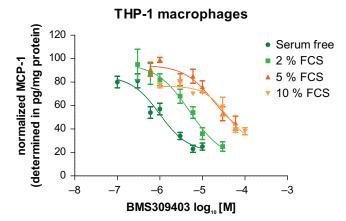
RESULTS

In vitro characterization of BMS309403—cellular efficacy in lowering secretion of MCP-1 from differentiated THP-1 macrophages

The potent FABP4 inhibitor BMS309403[23] has been shown to lower MCP-1 secretion from THP-1 macrophages.[12] However, the cellular efficacy of BMS309403 in this assay with an approximate IC_{50} of 25 μM[12] has been demonstrated to be low compared to the biochemical assay ($K_i < 2$ nM).[23] We therefore evaluated whether the efficacy of BMS309403 in the cellular setting is limited by high protein binding of the inhibitor to link maximal achievable cellular efficacy with the PK properties and

tissue exposure levels of BMS309403. We confirm the previously reported findings and demonstrate that the inhibitor is able to inhibit the secretion of the inflammatory chemokine in a dose-dependent manner. Using the protein-free cell culture medium HL-1, BMS309403 inhibits MPC-1 secretion with an IC_{50} of 1 μM. However, its efficacy is limited by protein binding, as shown by the IC_{50} shift under conditions of different FCS concentrations during treatment (**Fig. 1**). The respective IC_{50} values under these conditions are 1 μM (serum free), 5 μM (2% FCS), 19 (5% FCS), and 35 μM (10% FCS).

PK profile and in vivo tissue exposure of BMS309403 confirm that the drug reached its target site

The PK profile of the FABP4 inhibitor BMS309403 was determined in ob/ob mice after oral gavage of 40 mg/kg. The FABP4 inhibitor showed a C_{max} of 5880 nM with a t_{max} of 0.67 h, an AUC (nM × h) of 23 300, and mean residence time of 13 h. Adipose tissue levels were 838 nM 1 h postdosing and 986 nM 3 h following dosing of 40 mg/kg BMS309403. The data indicate that the plasma exposure levels exceeded the levels in the adipose tissue, at least during the first 3 h following administration of the drug.

FIG. 1. FABP4 inhibition dose-dependently inhibits secretion of the proinflammatory chemokine MCP-1 from THP-1 macrophages. THP-1 macrophages were treated with the FABP4 inhibitor for 24 h in medium with different concentrations of serum as described. MCP-1 level was determined in supernatants by enzyme-linked immunosorbent assay and normalized to protein. FCS, fetal calf serum.

In vivo lipidomics analysis identifies biomarker

In the discovery study, we aimed to analyze effects of BMS309403 on plasma metabolites in an acute setting after day 2 of treatment. We identified a set of metabolic traits that associated highly with dosage, even after Bonferroni correction for multiple testing (**Table 1** and **Fig. 2A**). The top-ranking metabolite pairs that were significantly and dose-dependently affected by drug treatment are ratios between phospholipids with lipid side chains from the C16:0, C16:1, C18:0, and C18:1 pool and C20:3, C20:4, and C22:4 polyunsaturated fatty acids (PUFAs). The time after the last drug administration—1 or 3 h postdosing—did not reveal any significant differences in the metabolite profile. Based on this outcome, a replication of the acute setup was performed to confirm the initial observations and to extend our findings toward analysis of adipose tissue. Besides macrophages, adipose tissue represents the primary target tissue for FABP4 inhibitors. In the replication setup, sampling of plasma and tissue was performed only at one time point (2 hours postdosing) because the initial experiment did not reveal differences in metabolite pattern between 1 and 3 h following drug administration. Furthermore, an additional vehicle control was included in the experiment to compare the commonly used 0.5% natrosol with the vehicle that has been specifically used to achieve high exposure for BMS309403.[12] In the replication setup, again BMS309403 significantly shifted the lipid balance between metabolite pairs for the C16:0, C16:1, C18:0, and C18:1 pool and C20:3, C20:4, and C22:4 PUFAs in plasma of mice independent of the vehicle that was used as a comparator (**Fig. 2B**).

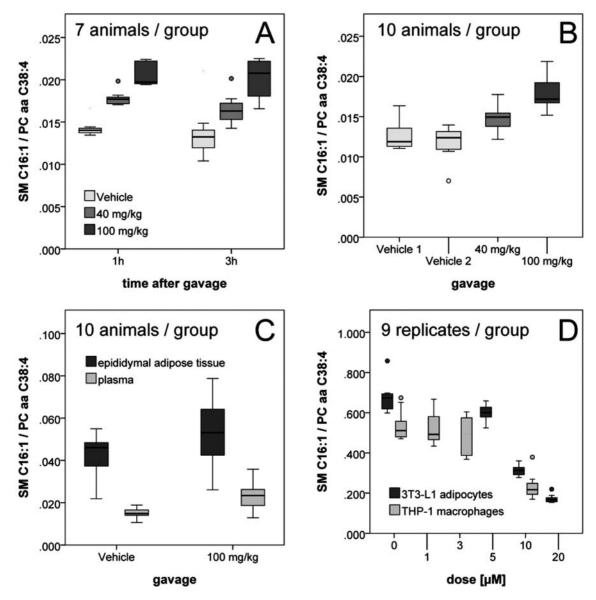### The same biomarker is also identified in adipose tissue

In an independent replication setup, epididymal adipose tissue was analyzed by lipidomics analyses for the effects of the FABP4 inhibitor BMS309403. As shown in **Figure 2C**, when compared to plasma samples from the same animals at the example metabolite ratio SM C16:1/PC aa C38:4, this metabolic trait was also upregulated in adipose tissue samples.

In vitro lipidomics analysis of supernatants from THP-1 macrophages and 3T3L1 adipocytes

As determined from the dose-dependent lowering of MCP-1 secretion from THP-1 macrophages, the efficacy of the FABP4 inhibitor in vitro is affected by protein binding. On the basis of our findings, we therefore performed all cellular treatments with the FABP4 inhibitor under serum-free conditions to achieve the highest potency possible. Treatment of THP-1 macrophages and 3T3L1 adipocytes was performed with concentrations of the inhibitor that were previously shown to affect MCP-1 secretion and fatty acid uptake, respectively.[12] For both cell lines, we identified metabolite pairs that were significantly and dose-dependently affected by drug treatment. In particular, lipid pairs between sphingomyelins with C16:1 and C18:1 lipid side chains on one side and PUFA side chains (i.e., arachidonate) on the other were identified. Based on the abundance of the respective fatty acids in cells and the substrate commonly found to bind to FABP4,[24] these data indicated that the inhibitor leads to a shift in lipid metabolites and their respective ratios. The most significantly affected metabolite pairs in vivo partially overlapped with the effects seen in vitro. However, the direction of deregulation for those metabolite pairs (e.g., SM C16:1/PC aa C38:4) was in an opposite direction as compared to the observation made in vivo in plasma and adipose tissue samples (**Fig. 2D**).
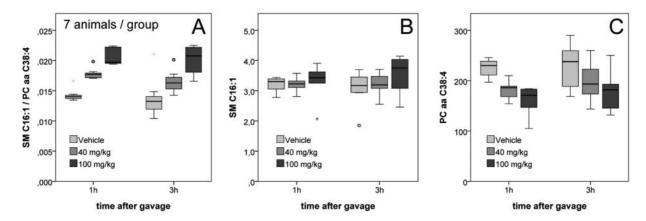
DISCUSSION

Here we describe our findings toward the identification of a potential biomarker for assessing acute in vitro and in vivo efficacy for the FABP4 inhibitor BMS309403.[12,23] With the identified in vivo plasma biomarker that reflects an acute drug action one day after start of treatment, we demonstrate the feasibility of such a lipidomics approach. Among the many significantly affected metabolite ratios, SM C16:1/PC aa C38:4 showed the most consistent and strongest associations with drug treatment, along with a number of other, biochemically closely related metabolite pairs, such as SM C18:1/PC aa C38:4 and SM C18:0/PC aa C38:5 (**Table 1**). The top-ranking metabolite pairs that were significantly and dose-dependently affected by drug treatment are ratios between phospholipids with lipid side chains from the C16:0, C16:1, C18:0, and C18:1 pool and C20:3, C20:4, and C22:4 PUFAs. This conclusion is based on the following

FIG. 2. The FABP4 inhibitor BMS309403 consistently alters the metabolite ratio SM C16:1/PC aa C38:4 in vivo and in vitro. (**A**) Dose-dependent effect of BMS309403 in plasma samples and independency of time after gavage; (**B**) replication and independence of type of vehicle; (**C**) ratio is altered in plasma and epididymal adipose tissue and (**D**) in 3T3-L1 adipocytes and THP-1 macrophages. However, in cell lines, the dose-dependent effect is inversely to the observation made in the in vivo plasma and adipose tissue samples.

reasoning (**Fig. 4**): although the precise position of the double bonds and the distribution of the carbon atoms in different fatty acid side chains cannot be explicitly determined with the technology we use here, based on knowledge of the predominant PUFAs in the human body and previous experience with the AbsoluteIDQ kit in genetic association studies with PUFA-related enzymes (*FADS1*, *ELOVL2*; see Illig et al.[14]), the major portion of the phosphocholines with four or five double bonds contains polyunsaturated fatty acid from the ω-3 and ω-6

pathways. For instance, the side chains of metabolite PC aa C38:4 are most likely composed of a major part of (C16:0,C20:4) and (C16:1,C20:3) fatty acid side chain pairs, albeit minor contributions of combinations such as (C14:0,C22:4) may also be present. It is clear that all metabolites that are found in the denominator of a ratio (PC aa C36:4, PC aa C38:4, PC aa C38:5, PC ae C38:3, PC ae C38:4, PC ae C40:4, lysoPC a C20:3 in **Table 1**) are likely to be composed of a combination of one saturated or mono-unsaturated fatty acid of chain length C16 or

FIG. 3. The use of ratios between metabolite concentrations may lead to a strong reduction in the overall variance and a corresponding improvement in the strength of association. Dose-dependent effect of BMS309403 in plasma samples and independency of time after gavage on (**A**) metabolite ratio SM C16:1/PC aa C38:4, (**B**) numerator metabolite concentrations of SM C16:1, and (**C**) denominator PC aa C38:4.
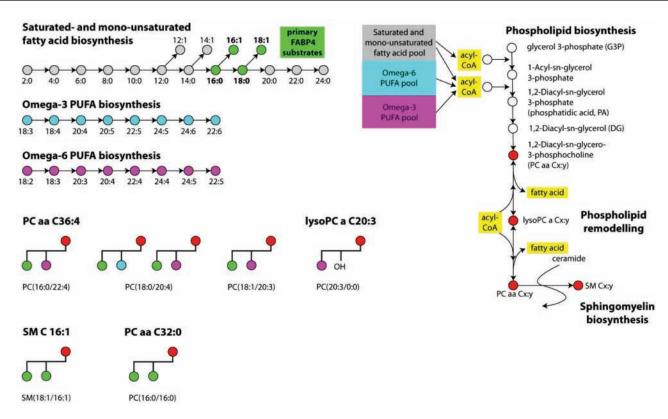
C18 and of one PUFA (except for lysoPC a C20:3, which carries a single PUFA side chain). In contrast, the metabolites that are found in the numerator of the ratios (PC aa C30:0, PC aa C30:2, PC aa C32:0, PC ae C34:1, SM C16:0, SM C16:1, SM C18:0, SM C18:1 in **Table 1**) all contain at least one saturated or mono-unsaturated fatty acid of chain length C16 or C18 but no PUFAs. Thus, the abundance of phospholipids that carry a PUFA in their side chains decreases with increasing dosage and therefore FABP4 inhibition, relative to the abundance of phospholipids that contain solely C16 and C18 fatty acids.

These C16 and C18 fatty acid species not only are highly abundant in adipose tissue as the primary target tissue but have been characterized as FABP4 ligands.[24] Recently, analysis of FABP4/5-deficient mice by a lipidomics analysis identified elevated levels for palmitoleate (C16:1n7) in the plasma of those animals.[13] It was demonstrated that palmitoleate is the main driver for the metabolic phenotype associated with deficiency of the FABP isoforms[13] that has been well characterized in various animal models for T2D and atherosclerosis.[25,26] Our attempt to apply palmitoleate as a reliable marker for drug action was not successful. One potential explanation might be the fact that acute inhibition of FABP4 might not sufficiently modulate palmitoleate levels to the extent as seen in conventional knockout animals. This is especially true considering that the inhibitor might not efficiently inhibit both FABP4 and 5 to be comparable to the "lipokine" that was identified in FABP4/5 double-knockout mice.

On the basis of the evidence we have presently at hand, we cannot yet formulate a precise hypothesis on the function of FABP4 or the consequences of its inhibition. However, our findings imply that inhibition of FABP4 triggers a shift in fatty acid fluxes of particular species—a shift that can be followed and applied to characterize the efficacy of FABP4 inhibitors in vitro

and, more important, acutely in vivo. In particular, this shift appears functionally related to the action of BMS309403. Our conclusion is supported by the in vivo PK data and especially adipose tissue exposure of BMS309403, where levels up to 1 µM were achieved. This dose is sufficient to show efficacy in a cellular model for FABP4 inhibition where half-maximal inhibition of MCP-1 from THP-1 macrophages was achieved. Moreover, although showing the reverse direction of regulation in vitro, there was an overlap between in vivo and in vitro metabolite pairs that were affected by the drug, which provides confidence regarding the specificity for a drug treatment–mediated effect. Although we cannot completely rule out that the acute action of BMS309403 on the lipid profile is due to "off-target" effects, various data sets provide evidence for an on-target, FABP4-dependent activity of the drug. First, BMS309403 has been characterized in vitro and in vivo in cells and animals lacking FABP4, where no drug action has been observed on the relevant readouts.[12] In addition, a gene array study that was performed by the authors in 3T3L1 adipocytes (data not shown, manuscript in preparation) identified a significant overlap between mRNAs that were deregulated after FABP4 inhibition and siRNA-mediated knockdown. In addition, BMS309403 did not reveal a clear "off-target" effect when assessed in a hit-profiling screen (**Supplemental Table 3**).

The reverse direction of deregulation and lower efficacy (half-maximal effect at 10 µM) might be attributed to the difference between the in vitro and in vivo situation. In contrast to the cellular test system, in vivo, continuous crosstalk between plasma and tissues might be one contributing factor that could explain the reverse direction of regulation. In addition, the cellular system might not be adequately equipped to reflect the rather complex situation of lipid handling in vivo to show the same drug response for this particular metabolite pair.

FIG. 4. Schematic view of the central pathways that are involved in the metabolism of the phospholipids investigated in this study. Top left: fatty acids are produced in the human body predominantly either by de novo synthesis from 2-carbon units, leading principally to saturated and mono-unsaturated even-sized fatty acids (gray), or starting from essential ω-3 fatty and ω-6 fatty acids, producing polyunsaturated fatty acids (PUFAs) of only specific carbon chain compositions (cyan and magenta). C16 and C18 fatty acids, which are the primary substrates of FABP4, are highlighted in green. Right: de novo phospholipid biosynthesis occurs in the Kennedy pathway (PUFAs are mainly attached to the *sn*-2 position of the glycerol moiety); existing phospholipids are remodeled by exchange of their lipid side chains and head groups; phospholipids that are measured by the technology used in this study are highlighted in red (PC aa Cx:y, PC ae Cx:y, lysoPC a Cx:y, SM C:x:y; see **Supplemental Table 1** for full names). Bottom left: examples of possible side chain compositions of selected metabolites presented in **Table 1**; note that only the most likely side chain compositions are shown. Other combinations are also present in the mixture, including fatty acids not listed here (e.g., issued from nutritional input); however, these contributions can be considered minor compared to the ones presented here.

Thus far, to our knowledge, this is the first attempt to apply lipidomics analysis toward the identification of an in vivo marker for FABP4 inhibition. One advantage of our approach of determining metabolite ratios rather than single metabolites is that they provide a highly reproducible and robust measure that does not require any particular standardization. Potential efficacy markers may be implemented by high-throughput FIA-MS/MS methods for the specific metabolite pairs of interest in terms of screening only a few MRM pairs. Application of machine learning techniques on these data may then be used to optimize the predictive value of the marker. This would allow a convenient and fast characterization of inhibitors in vitro and in vivo.

In summary, we are confident that the identified biomarker described here reflects drug treatment effects and believe that this marker can be attributed to FABP4 inhibition. In a next step, it remains to be shown whether the identified metabolite pair represents an acute mechanistic marker that is predictive of the long-term effect of FABP4 inhibition that ultimately translates into antidiabetic and antiatherosclerotic efficacy.

REFERENCES

1. Erion, DM, Shulman GI: Diacylglycerol-Mediated Insulin Resistance. *Nat. Med*. **2010**, *16*, 400–402.

2. Pratico, D, Dogne JM: Vascular Biology of Eicosanoids and Atherogenesis. *Expert Rev. Cardiovasc. Ther*. **2009**, *7*, 1079–1089.

3. Cowart, L. A. Sphingolipids: Players in the Pathology of Metabolic Disease. *Trends Endocrinol. Metab*. **2009**, *20*, 34–42.

4. Prieur, X.; Roszer, T.; Ricote, M. Lipotoxicity in Macrophages: Evidence from Diseases Associated with the Metabolic Syndrome. *Biochim. Biophys. Acta* **2010**, *1801*, 327–337.

5. Furuhashi, M.; Hotamisligil, G. S. Fatty Acid–Binding Proteins: Role in Metabolic Diseases and Potential as Drug Targets. *Nat. Rev. Drug Discov*. **2008**, *7*, 489–503.

6. Hotamisligil, G. S.; Johnson, R. S.; Distel, R. J.; Ellis, R.; Papaioannou, V. E.; Spiegelman, B. M. Uncoupling of Obesity from Insulin Resistance through a Targeted Mutation in aP2, the Adipocyte Fatty Acid Binding Protein. *Science* **1996**, *274*, 1377–1379.

7. Uysal, K. T.; Scheja, L.; Wiesbrock, S. M.; Bonner-Weir, S.; Hotamisligil, G. S. Improved Glucose and Lipid Metabolism in Genetically Obese Mice Lacking aP2. *Endocrinology* **2000**, *141*, 3388–3396.

8. Makowski, L.; Brittingham, K. C.; Reynolds, J. M.; Suttles, J.; Hotamisligil, G. S. The Fatty Acid–Binding Protein, aP2, Coordinates Macrophage Cholesterol Trafficking and Inflammatory Activity: Macrophage Expression of aP2 Impacts Peroxisome Proliferator-Activated Receptor gamma and IkappaB Kinase Activities. *J. Biol. Chem*. **2005**, *280*, 12888–12895.

9. Makowski, L.; Boord, J. B.; Maeda, K.; Babaev, V. R.; Uysal, K. T.; Morgan, M. A.; Parker, R. A.; Suttles, J.; Fazio, S.; Hotamisligil, G. S.; et al. Lack of Macrophage Fatty-Acid-Binding Protein aP2 Protects Mice Deficient in Apolipoprotein E against Atherosclerosis. *Nat. Med*. **2001**, *7*, 699–705.

10. Lehmann, F.; Haile, S.; Axen, E.; Medina, C.; Uppenberg, J.; Svensson, S.; Lundback, T.; Rondahl, L.; Barf, T. Discovery of Inhibitors of Human Adipocyte Fatty Acid–Binding Protein, a Potential Type 2 Diabetes Target. *Bioorg. Med. Chem. Lett*. **2004**, *14*, 4445–4448.

11. Ringom, R.; Axen, E.; Uppenberg, J.; Lundback, T.; Rondahl, L.; Barf, T. Substituted Benzylamino-6-(trifluoromethyl)pyrimidin-4(1H)-ones: A Novel Class of Selective Human A-FABP Inhibitors. *Bioorg. Med. Chem. Lett*. **2004**, *14*, 4449–4452.

12. Furuhashi, M.; Tuncman, G.; Gorgun, C. Z.; Makowski, L.; Atsumi, G.; Vaillancourt, E.; Kono, K.; Babaev, V. R.; Fazio, S.; Linton, M. F.; et al. Treatment of Diabetes and Atherosclerosis by Inhibiting Fatty-Acid-Binding Protein aP2. *Nature* **2007**, *447*, 959–965.

13. Cao, H.; Gerhold, K.; Mayers, J. R.; Wiest, M. M.; Watkins, S. M.; Hotamisligil, G. S. Identification of a Lipokine, a Lipid Hormone Linking Adipose Tissue to Systemic Metabolism. *Cell* **2008**, *134*, 933–944.

14. Illig, T.; Gieger, C.; Zhai, G.; Romisch-Margl, W.; Wang-Sattler, R.; Prehn, C.; Altmaier, E.; Kastenmuller, G.; Kato, B. S.; Mewes, H. W.; et al. A Genome-Wide Perspective of Genetic Variation in Human Metabolism. *Nat. Genet*. **2010**, *42*, 137–141.

15. Gieger, C.; Geistlinger, L.; Altmaier, E.; Hrabe de Angelis, M.; Kronenberg, F.; Meitinger, T.; Mewes, H. W.; Wichmann, H. E.; Weinberger, K. M.; Adamski, J.; et al. Genetics Meets Metabolomics: A Genome-Wide Association Study of Metabolite Profiles in Human Serum. *PLoS Genet*. **2008**, *4*, e1000282.

16. Verollet, R. A Major Step towards Efficient Sample Preparation with Bead-Beating. *Biotechniques* **2008**, *44*, 832–833.

17. Hettick, J. M.; Green, B. J.; Buskirk, A. D.; Kashon, M. L.; Slaven, J. E.; Janotka, E.; Blachere, F. M.; Schmechel, D.; Beezhold, D. H. Discrimination of Aspergillus Isolates at the Species and Strain Level by Matrix-Assisted Laser Desorption/Ionization Time-of-Flight Mass Spectrometry Fingerprinting. *Anal. Biochem*. **2008**, *380*, 276–281.

18. Wu, H.; Southam, A. D.; Hines, A.; Viant, M. R. High-Throughput Tissue Extraction Protocol for NMR- and MS-Based Metabolomics. *Anal. Biochem*. **2008**, *372*, 204–212.

19. Weinberger, K.M. Metabolomics in diagnosing metabolic diseases [in German]. *Ther. Umsch*. **2008**, *65*, 487–491.

20. Altmaier, E.; Ramsay, S. L.; Graber, A.; Mewes, H. W.; Weinberger, K. M.; Suhre, K. Bioinformatics Analysis of Targeted Metabolomics: Uncovering Old and New Tales of Diabetic Mice under Medication. *Endocrinology* **2008**, *149*, 3478–3489.

21. Wang-Sattler, R.; Yu, Y.; Mittelstrass, K.; Lattka, E.; Altmaier, E.; Gieger, C.; Ladwig, K. H.; Dahmen, N.; Weinberger, K. M.; Hao, P.; et al. Metabolic Profiling Reveals Distinct Variations Linked to Nicotine Consumption in Humans: First Results from the KORA Study. *PLoS One* **2008**, *3*, e3863.

22. Storey, J. D. The Positive False Discovery Rate: A Bayesian Interpretation and the q-Value. *Ann. Stat*. **2003**, *31*, 2013–2035.

23. Sulsky, R.; Magnin, D. R.; Huang, Y.; Simpkins, L.; Taunk, P.; Patel, M.; Zhu, Y.; Stouch, T. R.; Bassolino-Klimas, D.; Parker, R.; et al. Potent and Selective Biphenyl Azole Inhibitors of Adipocyte Fatty Acid Binding Protein (aFABP). *Bioorg. Med. Chem. Lett*. **2007**, *17*, 3511–3515.

24. Richieri, G. V.; Ogata, R. T.; Kleinfeld, A. M. Equilibrium Constants for the Binding of Fatty Acids with Fatty Acid–Binding Proteins from Adipocyte, Intestine, Heart, and Liver Measured with the Fluorescent Probe ADIFAB. *J. Biol. Chem*. **1994**, *269*, 23918–23930.

25. Maeda, K.; Cao, H.; Kono, K.; Gorgun, C. Z.; Furuhashi, M.; Uysal, K. T.; Cao, Q.; Atsumi, G.; Malone, H.; Krishnan, B.; et al. Adipocyte/Macrophage Fatty Acid Binding Proteins Control Integrated Metabolic Responses in Obesity and Diabetes. *Cell Metab*. **2005**, *1*, 107–119.

26. Boord, J. B.; Maeda, K.; Makowski, L.; Babaev, V. R.; Fazio, S.; Linton, M. F.; Hotamisligil, G. S. Combined Adipocyte-Macrophage Fatty Acid–Binding Protein Deficiency Improves Metabolism, Atherosclerosis, and Survival in Apolipoprotein E-Deficient Mice. *Circulation* **2004**, *110*, 1492–1498.

Address correspondence to:
Karsten Suhre
Institute for Bioinformatics and Systems Biology
Helmholtz Zentrum München
German Research Center for Environmental Health
Ingolstädter Landstrasse 1, 85764 Neuherberg, Germany

E-mail: karsten.suhre@helmholtz-muenchen.de